

# Room Temperature Cured Hydrophobic Nano-Silica Coatings for Outdoor Insulators Installed on Power Lines without Shutting Down the Current

P. Soroori<sup>1</sup>, S. Baghshahi<sup>2,\*</sup>, A. Kazemi<sup>1</sup>, N. Riahi Noori<sup>3</sup>, S. Payrazm<sup>1</sup>, A. Aliabadizadeh<sup>1</sup>

\* baghshahi@eng.ikiu.ac.ir

<sup>1</sup> Department of Materials Engineering, Science and Research Branch, Islamic Azad University, Tehran, Iran

<sup>2</sup> Department of Materials Science and Engineering, Faculty of Engineering, Imam Khomeini International University, Qazvin, Iran

<sup>3</sup> Non-Metallic Materials Research Group, Niroy Research Institute, Tehran, Iran

Received: January 2022

Revised: April 2022

Accepted: May 2022

DOI: 10.22068/ijmse.2598

**Abstract:** The present study aims to prepare a room temperature cured hydrophobic and self-cleaning nano-coating for power line insulators. As a result, the installed insulators operating in power lines can be coated without being removed from the circuit and without the need to cut off power. For this purpose, hydrophobic silica nanoparticles were synthesized by the sol-gel method using TEOS and HMDS. The synthesized hydrophobic silica nanoparticles were characterized by XRD, FTIR, SEM, and TEM analyses to investigate phase formation, particle size, and morphology. Then the surface of the insulator was cleaned and sprayed with Ultrimeg binder solution, an air-dried insulating coating, as the base coating. Then the hydrophobic nano-silica powder was sprayed on the binder-coated surface and left to be air-cured at room temperature. After drying the layer, the contact angle was measured to be 149°. A pull-off test was used to check the adhesion strength of the hydrophobic coating to the base insulator. UV resistance and fog-salt corrosion tests were conducted to evaluate the effect of environmental factors. The results showed that 150 hours of UV radiation, equivalent to 9 months of placing the samples in normal conditions, did not significantly reduce the hydrophobicity of the applied coatings.

**Keywords:** Hydrophobic, Self-cleaning, Room temperature curing, Coatings, Silica nanoparticles, Insulator.

## 1. INTRODUCTION

The fabrication of self-cleaning nano-coating is one of the main developments in surface-modified materials. Applying this type of coating on insulators used in different environments with harsh weather conditions, especially in highly polluted areas, can strongly contribute to the elimination of the flashover phenomenon. That is one of the main problems of insulators in polluted and moist areas [1-4].

The occurrence of some phenomena such as widespread dust storms, slight rainfalls, decreased wind, and muggy weather reduces the insulator's breakdown voltage and leads to dry surface band arcing and flash overdue to the inevitably increased creepage current (leakage current). This can cause a power outage and, consequently property damages or even casualties [5].

This research aims to produce a hydrophobic nano-silica coating, which is stable and applicable in-situ in a power supply line, at ambient temperature, without any heat treatment.

Hydrophilicity or hydrophobicity of the surface is

the desire for water molecules to bind with atoms or molecules of the surface via physical or hydrogen bonds. When a water droplet thoroughly wets the surface or becomes adsorbed, it will have a zero contact angle with the substrate. The surface, which tends to bind with the water molecules and adsorb them, is called a hydrophilic surface. Hydrophilic materials have polar bonds and molecules just like water. Appositely, when water does not wet the surface or completely is rejected by the surface, it will have a contact angle of about 180° with the substrate. The surface, which does not tend to bind with the water molecules and rejects them, is called a hydrophobic surface. Hydrophobic materials usually have non-polar bonds. Fig. 1 represents a 2D sketch of different states of the interaction between a water droplet and the surface [6-9].

According to Fig. 1, water is distributed on the hydrophilic surface, and the contact angle between the surface and water is less than 90°, and the surface becomes wet. In this state, the water-soluble pollutants on the surface find better conditions for dissolution in water and removal

from the surface with the current water flow. But on a hydrophobic surface, a water droplet rolls on the surface, separates the pollutants and removes them. Fig. 2 shows the schematics of a hydrophilic surface with a conical roughness in collision with a water droplet over time [7, 10, 11].

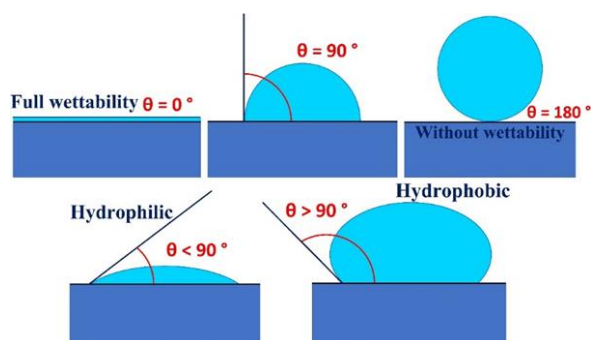


**Fig. 1.** The different states of the interaction between a water droplet and the surface.

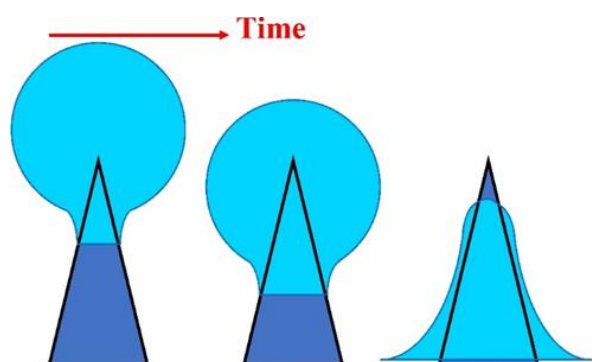


**Fig. 2.** Schematics of a hydrophilic surface with a conical roughness in collision with a water droplet over time.

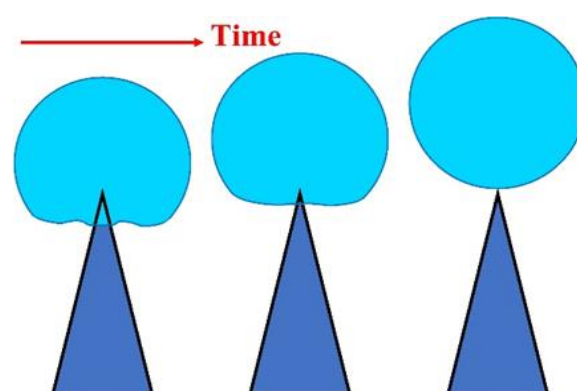
According to Fig. 2, if the surface is hydrophilic, the contact angle decreases with the increase of surface roughness. In other words, a water layer is formed on the surface, and the contact between water and the basic surface increases as much as possible.

Fig. 3 shows the schematics of a hydrophobic surface with a conical roughness in collision with a water droplet over time.

According to Fig. 3, if the surface is hydrophobic, the contact angle increases with the increase of surface roughness. The water molecules accumulate and become spherical as much as possible. This form decreases contact between water and the surface to the minimum level [4, 15-17].

This research aims to produce a hydrophobic nano-silica coating, which is stable and applicable in-situ in a power supply line, at ambient temperature, without any heat treatment, and without the need for power cut-off.

In this study, without any heat treatment, a stable hydrophobic and self-cleaning coating was applied on the surface of installed insulators operating in power lines. This coating can be applied without removing the circuit and needing to cut off power. As a result, in addition to the low cost of this method, ancillary costs caused by shutting down the power line are also avoided.



**Fig. 3.** Schematics of a hydrophobic surface with a conical roughness in collision with a water droplet over time.

## 2. EXPERIMENTAL PROCEDURE

### 2.1. Materials

The raw materials for the synthesis of hydrophobic nano-silica powder were high purity Tetraethyl orthosilicate (Sigma-Aldrich 333859), Ammonium Hydroxide (Sigma-Aldrich 338818), Hydroxytyramine Hydrochloride (Sigma-Aldrich H8502), Hexamethyldisilazane (Sigma-Aldrich H8502), Ethanol (Sigma-Aldrich 32221-M), and Ultimeg<sup>1</sup> binder.

### 2.2. Synthesis of hydrophobic nano-silica powder

The sol-gel method was used for the synthesis of hydrophobic nano-silica powder. 4 mL of TEOS solution was mixed with 50 mL ethanol and was magnetically stirred for 10 min until full homogenization was achieved. Then, 3 mL ammonium hydroxide was added to the solution, and it was magnetically stirred for 5 hours at room

<sup>1</sup> Ultimeg 2000/372, Anti-tracking Varnish GOLDEN

Q.D., Advanced Electrical Varnishes, U.K.

temperature. Then, 0.3 g dopamine hydrochloride and 8 mL HMDS<sup>2</sup> were added to the solution while stirring. After one hour, the hydrolysis reaction between TEOS and HMDS was completed. The solution was dried at 110°C.

The dried powder was washed twice with ethanol. After drying, the hydrophobic nano-silica powder containing the brown HMDS-dopamine hydrochloride particles was obtained. Fig. 4 shows the hydrophobic nano-silica powder synthesis flowchart.

### 2.3. Applying the hydrophobic coating

Initially, the surface of the substrate was washed with water and dried. Ultimeg binder was used as the base coating to avoid electrical leakage and to provide moisture resistance. The binder was sprayed to the surface from a distance of 10 cm. Depending on the ambient temperature, sufficient time was given for the binder to set. Then the hydrophobic nano-silica powder was sprayed on the binder-impregnated surface, and the applied coating was well-dried after 6 hours at the environment temperature.

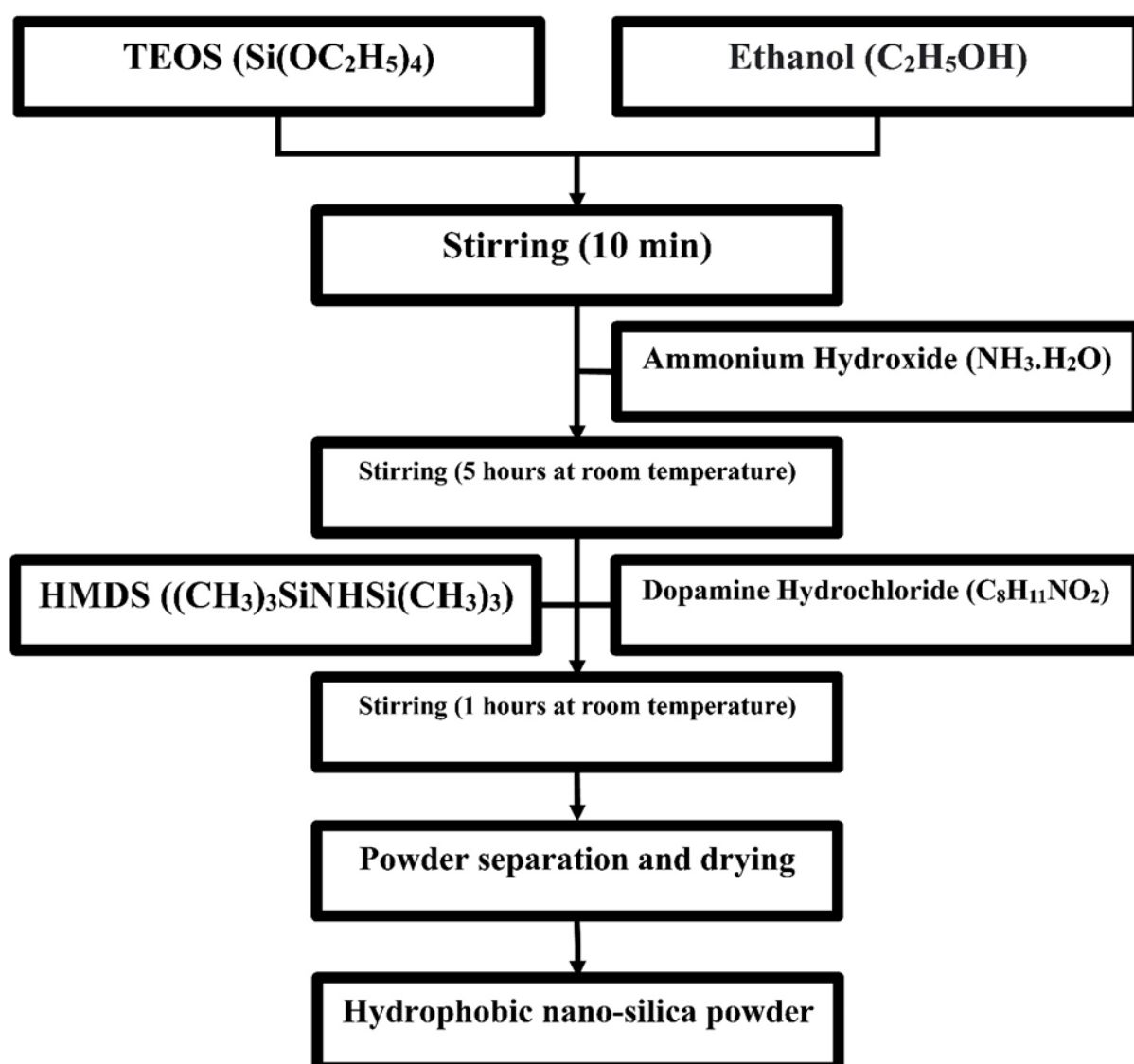


Fig. 4. Hydrophobic nano-silica powder synthesis flowchart.

<sup>2</sup>Hexamethyldisilazane (HMDS, (CH<sub>3</sub>)<sub>3</sub>SiNHSi(CH<sub>3</sub>)<sub>3</sub>)

## 2.4. Characterization

X-ray diffractometry (XRD, Philips PW 1730) was performed to determine the type of phases formed in the hydrophobic nano-silica. To ensure the formation of the desired atomic bonds, the hydrophobic nano-silica powder was examined by Fourier transform infrared spectroscopy (FTIR-BRUKER Vector 22). The morphology and size of the synthesized hydrophobic nano-silica powder was examined by scanning electron microscopy (SEM, FEI Quanta 200E) equipped with an elemental analysis system (EDS) and transmission electron microscopy (TEM, Philips EM 208S). Coated samples were observed by atomic force microscopy (ARA, AFM Vacuum Standard Model) to examine the surface topography. For testing the water contact angle, a small drop of water was gently placed on the surface and photographed using a microscope (VEHO USB Microscope 400x). To check the adhesion strength of the hydrophobic nano-silica coating on the surface, the pull-off test was performed at 23 °C and a humidity of 45% according to ASTM D4541. To increase the accuracy of the results, each pull-off test was repeated 4 times. A UV resistance test was performed by a carbon filament lamp at a 300 to 400 nm UV wavelength range and 20 W to investigate the effect of sunlight on the applied hydrophobic coating. The relative humidity of the laboratory environment was  $50 \pm 5$ , and the temperature was kept constant at 35 °C.

The test was performed using the "SHT-214D" device for 150 hours. According to ASTM standard, every 200 hours of exposure to the mentioned conditions is equivalent to 1 year of exposure of the sample to natural sunlight in working conditions. The nozzle of the spray resistance test device in fog-salt conditions was selected according to the "ASTM B117" standard. To create the test conditions, the spray device's nozzle was placed in the bottom of the chamber to ensure upward spraying and fog formed on the top of the sample.

The spraying was not done directly on the surface of the sample, and a solution with standard concentrations of deionized water and NaCl was used. Finally, after placing the samples in the mentioned standard conditions for 150 hours, the results were analyzed according to "ASTM

D714" and "ASTM D1654" standards. The fracture voltage test was performed in environmental conditions with a temperature of 25.5 °C, humidity of 35%, and a pressure of 875.3 hPa, five times according to IEC international standard.

## 3. RESULTS AND DISCUSSION

### 3.1. Phase determination of the synthesized hydrophobic nano-silica powder

Fig. 5 shows the X-ray diffraction patterns of the synthesized hydrophobic nano-silica powder. As observed in Fig. 5, only tetragonal silica phase with JCPDS No. 01-079-0430 in  $\alpha$ -cristobalite structure that has  $a = 20.0647$  Å,  $b = 20.0647$  Å,  $c = 13.4082$  Å and  $\alpha = \beta = \gamma = 90^\circ$  is specified.

The pattern has characteristic peaks at  $2\theta = 15^\circ$ ,  $23^\circ$ ,  $32^\circ$ , and  $46^\circ$ . The hill-like shape of the graph confirms that the silica powder is nano-sized (Fig. 7).

### 3.2. FTIR spectroscopy of the synthesized hydrophobic nano-silica powder

The obtained FTIR spectrum from the synthesized nano-silica powder is shown in Fig. 6.

As shown in Fig. 6, the observed peaks in the wavenumbers of  $467$   $\text{cm}^{-1}$ ,  $1637$   $\text{cm}^{-1}$ , and  $947$   $\text{cm}^{-1}$  are related to the moisture or the -Si-OH bonds. The determined peaks at  $800$   $\text{cm}^{-1}$  and  $1100$   $\text{cm}^{-1}$  are related to Si-O-Si and hydroxyl groups on SiO<sub>2</sub>. The peaks at  $3423$   $\text{cm}^{-1}$ ,  $2920$   $\text{cm}^{-1}$ , and  $1393$   $\text{cm}^{-1}$  are attributed to the hydrophobic OH, CH<sub>3</sub>, and Si-C bonds formed on SiO<sub>2</sub> as a result of Hexamethyldisilazane and dopamine with Tetraethyl orthosilicate. This indicates the optimal formation of hydrophobic functional groups on silica [3].

### 3.3. Microstructural investigation of the synthesized hydrophobic nano-silica powder

Fig. 7 shows the Scanning electron microscopy (SEM) images of the synthesized hydrophobic nano-silica powder in the Backscattered Electron mode (BSE).

According to Fig. 7, the diameter of the synthesized silica particles is less than 100 nm. The nano-sized nature of the synthesized hydrophobic silica is the reason for the XRD hill-like graph (Fig. 5).

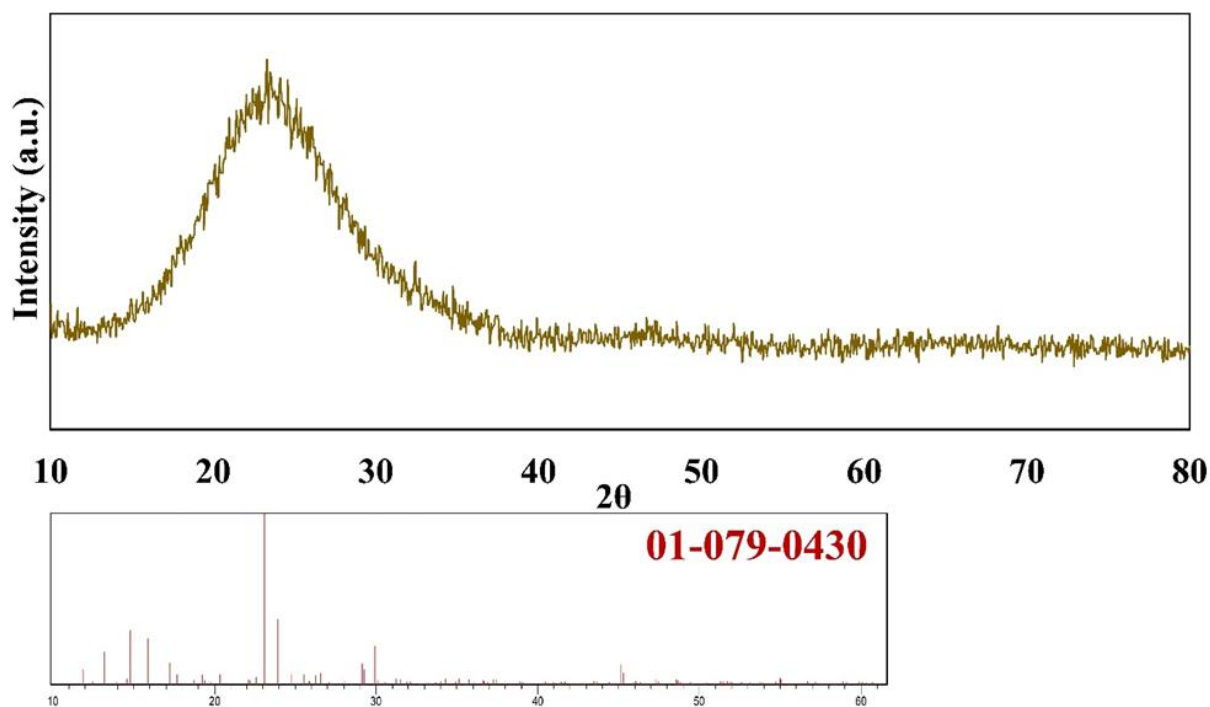


Fig. 5. XRD pattern of the synthesized hydrophobic nano-silica powder.

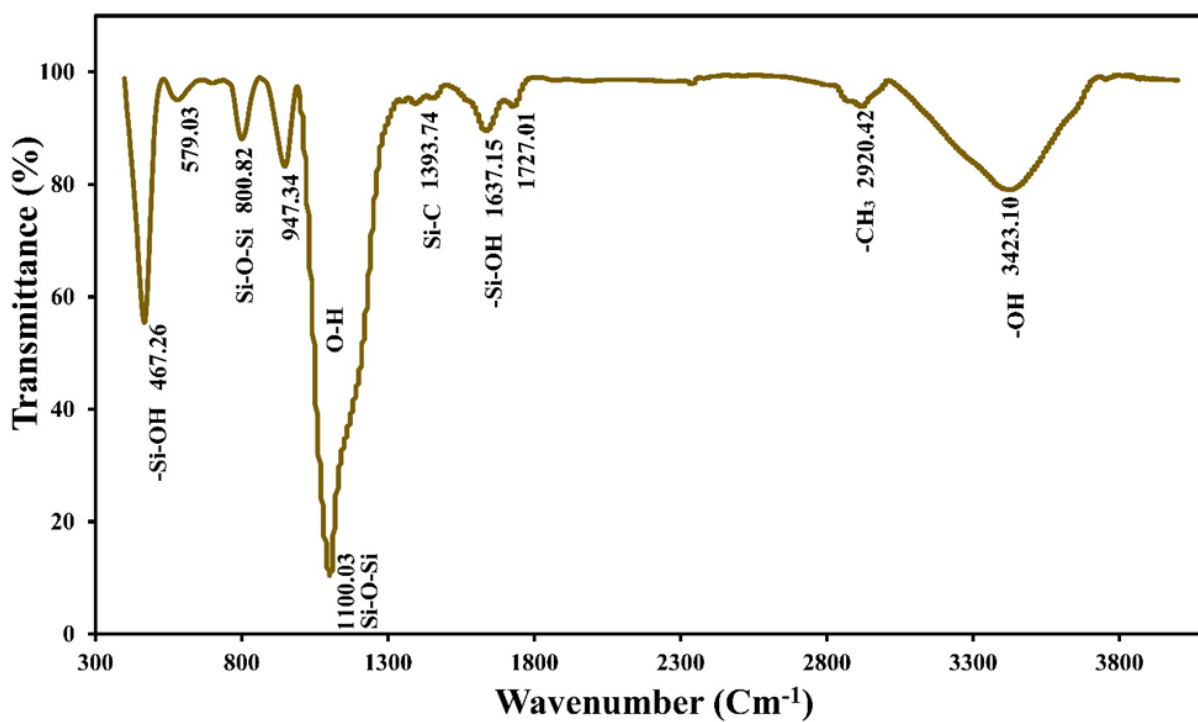


Fig. 6. FTIR spectrum of the synthesized nano-silica powder.

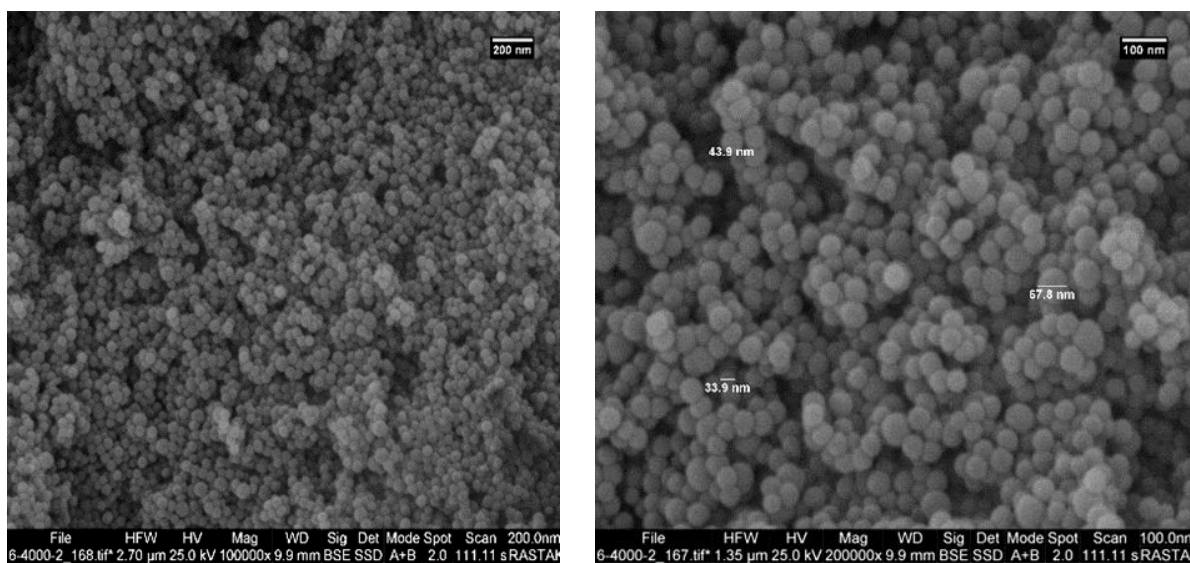


Fig. 7. SEM images of the synthesized hydrophobic nano-silica powder.

Fig. 8 shows the synthesized hydrophobic nano-silica sample analysis using the Energy-

Dispersive X-ray Spectroscopy (EDS) mode of the SEM microscope.

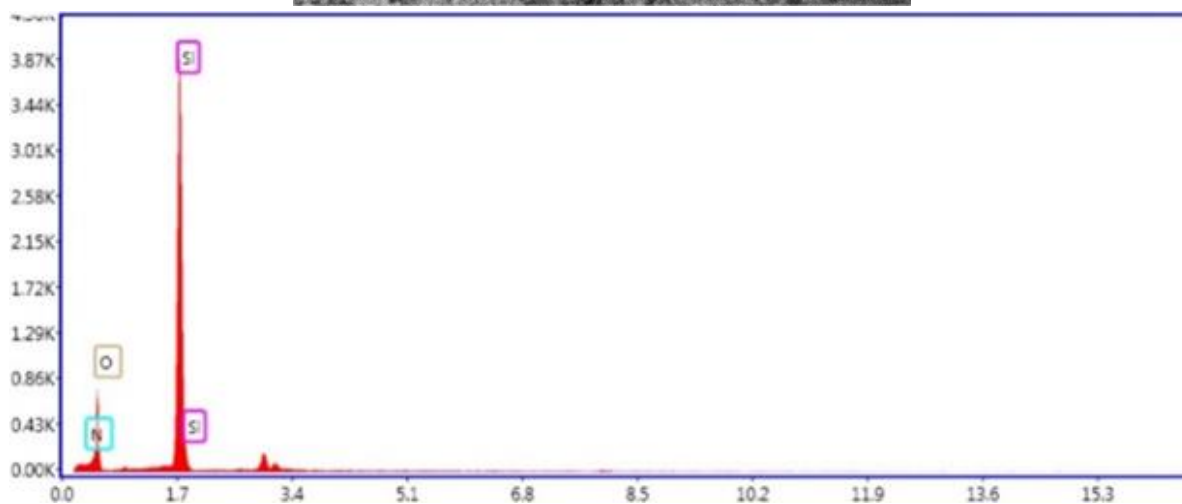
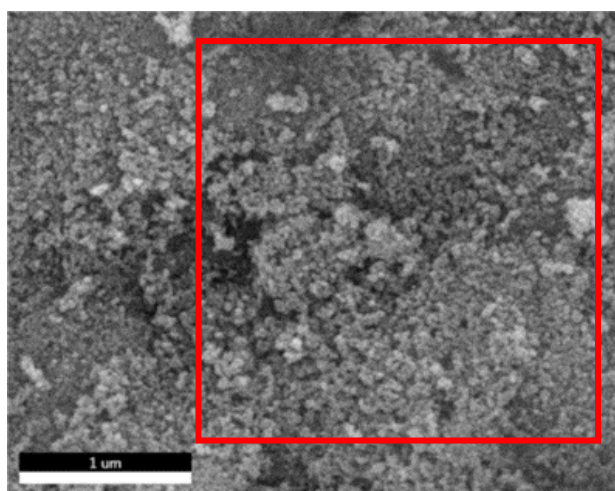
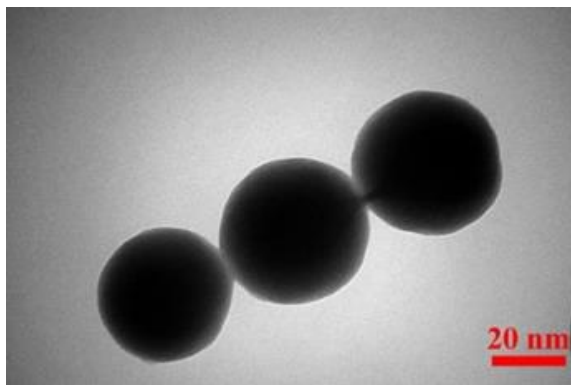


Fig. 8. EDS diagram of the synthesized hydrophobic nano-silica sample.

According to Fig. 8, the scanned area contains silicon, oxygen, and nitrogen. Table 1 shows the weight and atomic percentages of the obtained elements from the analysis in Fig. 8. According to table 1, the hydrophobic silica sample is synthesized without pollution.

Fig. 9 shows the Transmission Electron Microscope (TEM) image of the synthesized hydrophobic nano-silica powder. According to Fig. 9, the synthesized hydrophobic nano-silica particles were spherical, and their size was less than 100 nm. This spherical shape increases the powder flowability, leading to the suitable distribution of powder on the surface.



**Fig. 9.** TEM image of the synthesized hydrophobic nano-silica powder.

### 3.4. Microstructural investigation of the applied hydrophobic nano-silica coating

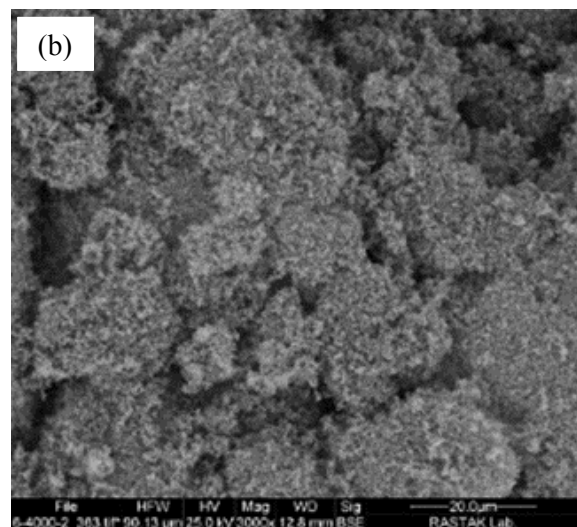
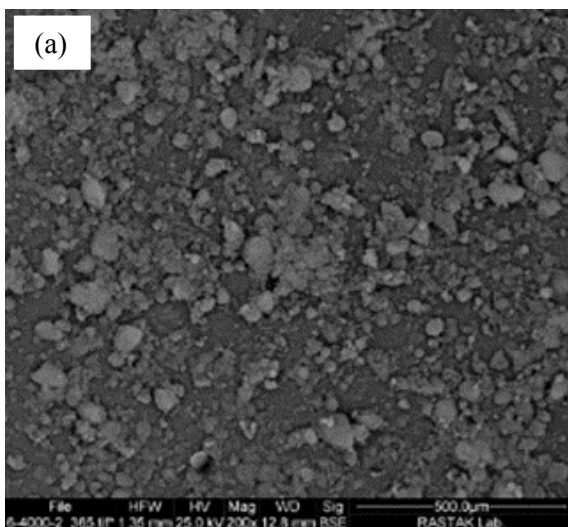
Fig. 10 shows the SEM images of the coated surface of the sample using the synthesized hydrophobic nano-silica powder in the Backscattered Electron mode. According to Fig. 10, the spray-coating process resulted in an appropriate and uniform coating. The porous layer increases the efficient contact surface and intensifies the hydrophobicity property.

Fig. 11 shows the SEM images of the cross-section of the coated sample by the synthesized hydrophobic nano-silica powder with Backscattered Electron mode. According to Fig. 11, the obtained coating tightly adheres to the ceramic substrate. Also, the thickness of the coating in this experiment is about 5 μm.

Fig. 12 shows the non-contact mode Atomic Force Microscopy (AFM) images of the sample's surface topography using the synthesized hydrophobic nano-silica powder. According to Fig. 12, the existing asperities on the coated surface are about 4 μm high. These asperities on the coated surface have increased the specific surface area and consequently the hydrophobicity property [3]. Using the spray method is one reason for forming such a surface with a controlled roughness.

**Table 1.** The weight and atomic percentages of the obtained elements from the EDS experiment.

Element	Atomic percentage	Weight percentage
Nitrogen	16.38	11.56
Oxygen	49.01	39.49
Silicone	34.61	48.95



**Fig. 10.** SEM images of the coated surface by the synthesized hydrophobic nano-silica powder in the environment (a) surface with 500 μm magnifying and (b) the same surface with 20 μm magnifying.

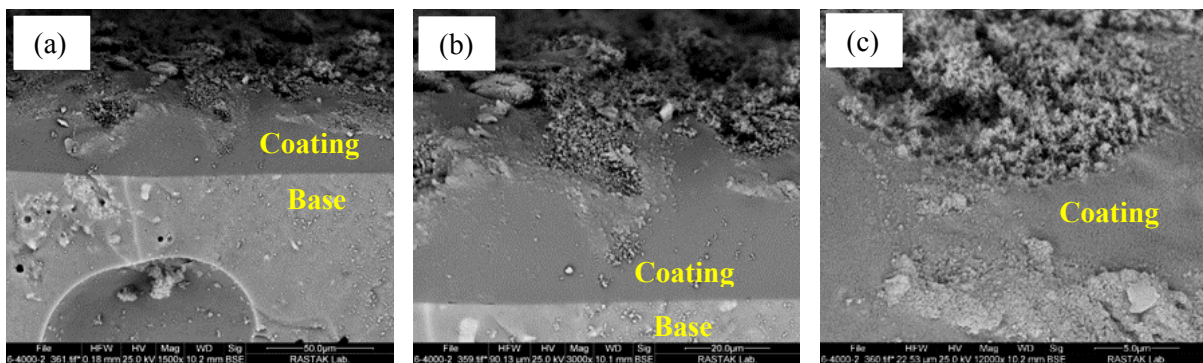


**Fig. 11.** SEM images of the cross-section of the coated sample by the synthesized hydrophobic nano-silica powder in the environment. (a) and (b) show the boundary between coated layer and base and (c) coated layer.

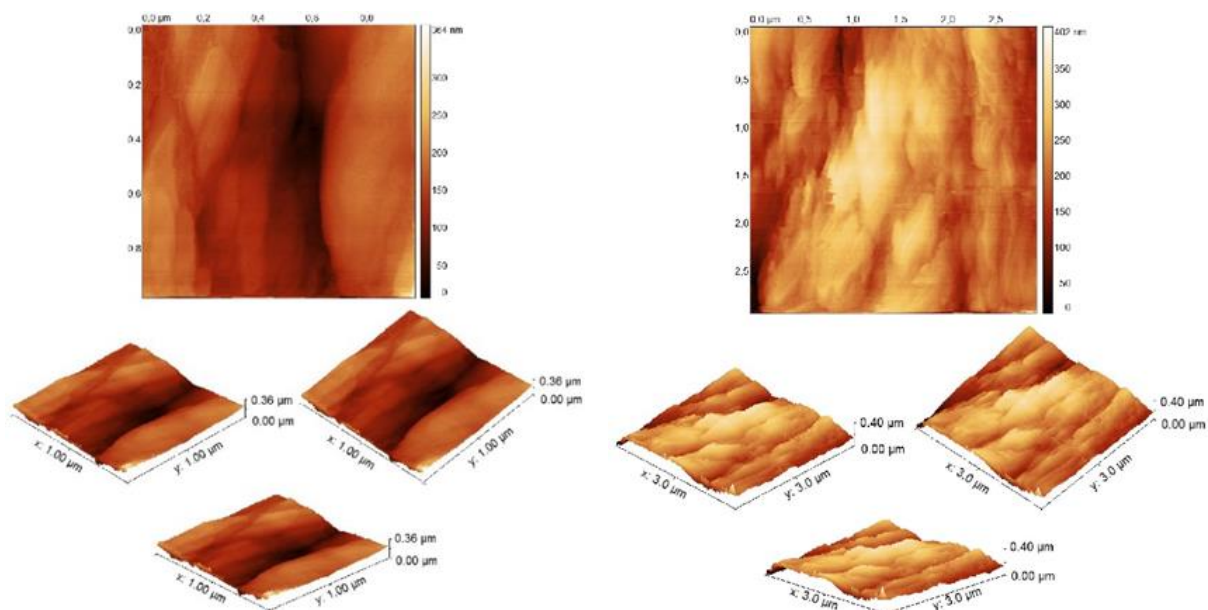


**Fig. 12.** The non-contact mode AFM images of the surface topography of the sample using the synthesized hydrophobic nano-silica powder.

### 3.5. Investigation of the coating properties

Fig. 13 shows the surface of the insulator after the adhesion strength test by the "pull-off" method with ASTM D4541.

The pull-off test was repeated 4 times to increase accuracy. According to Figs. 13 a and b, the adhesion strength of the uncoated and coated glazed insulator was 3.32 and 2.87 MPa, respectively, and the error coefficient was 0.015 MPa.

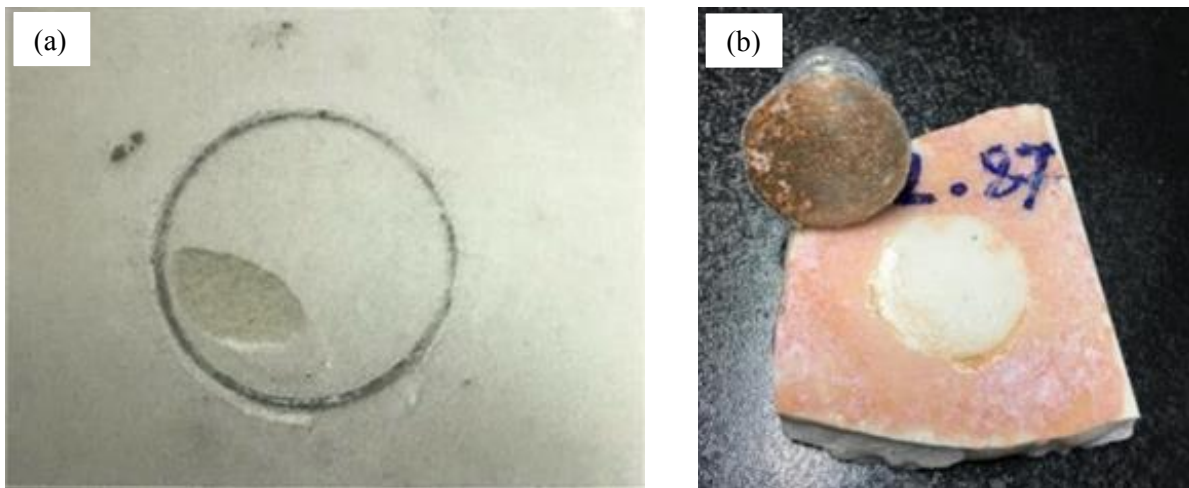
Fig. 14 shows the water contact angle of the coated surface before the UV radiation.

According to Fig. 14, the applied hydrophobic coating before UV radiation resulted in a water contact angle of 149°. Also, Fig. 14 shows the water contact angle of the coating after 150 h UV radiation in the SHT-214D device according to ASTM standard conditions.

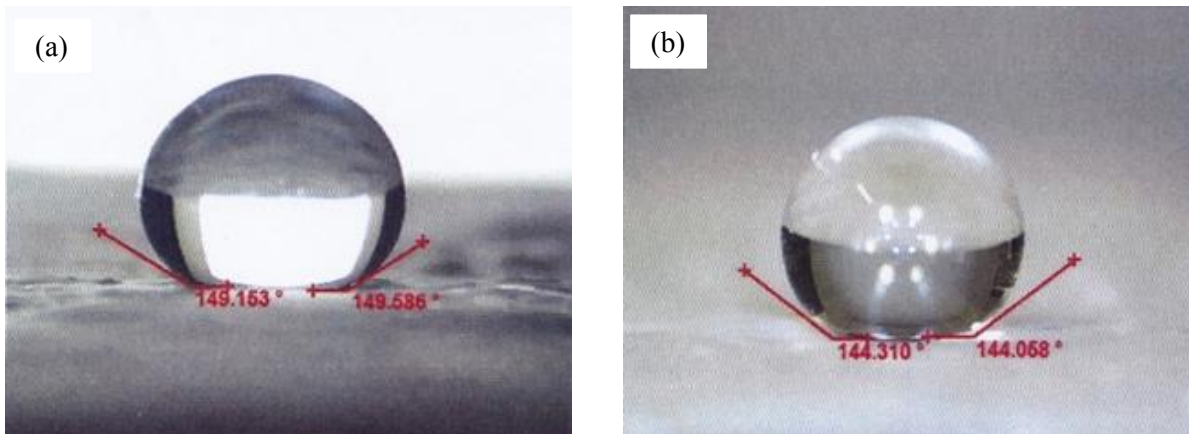
According to Fig. 14, 15 hours of exposure to UV radiation, which equals 9 months of exposure to the natural sunlight under working conditions, has decreased the contact angle of a droplet from 149° to 144°. The decrease of water contact angle under working conditions is negligible, indicating the appropriate stability of the applied coating under UV radiation.

Fig. 15 shows the coated sample after 150 hours of exposure to the salty-fog conditions according to ASTM-B117. According to Fig. 15, 150 hours of exposure to the conditions indicated in the standard ASTM B117 10% of the applied coating has remained, and the coating was detached from the substrate. The optimum life of the synthesized hydrophobic nano-silica coating is about 9 months under working conditions.





**Fig. 13.** The surface of the insulator after the adhesion strength test by the "pull-off" method (a) before coating and (b) after coating.



**Fig. 14.** The water contact angle of the coated surface (a) before UV radiation. (b) after 150 h UV radiation in SHT-214D device according to ASTM standard conditions.



**Fig. 15.** The coated sample after 150 hours of emplacement under the salty-fog conditions according to ASTM-B117.

Fig. 16 shows the breakdown voltage experiment on a KN120 insulator without coating according to the international standard of

IEC-60383-01.

Fig. 16 shows the breakdown voltage experiment according to the international standard of IEC-60383-01. According to this test, the safe voltage operating range that can be applied to the insulator without coating was 62 kV at the maximum point.

Fig. 17 shows the breakdown voltage experiment on a KN120 insulator with a coating according to the international standard of IEC-60383-01.

According to Fig. 17, the KN120 insulator coated with the hydrophobic nano-silica coating started sparking after 5 repeats of the experiment at an average voltage of 72 kV. Consequently, the applied hydrophobic nano-silica coating has improved insulator properties and increased the average required voltage for the initiation of sparking.



Fig. 16. The breakdown voltage experiment is according to the international standard of IEC-60383-01.

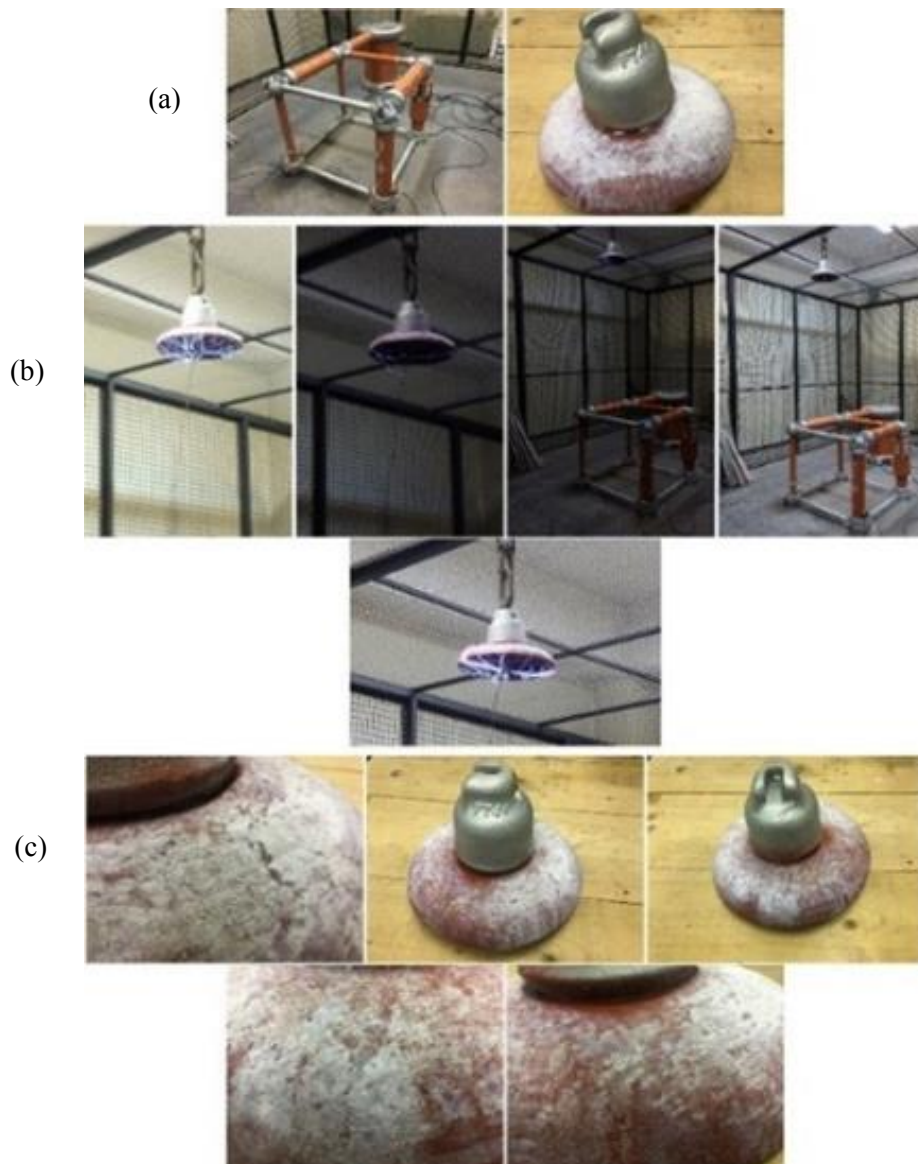


Fig. 17. The breakdown voltage experiment according to the international standard of IEC, (a) the coated insulator before the experiment, (b) voltage application on the insulator and increase of the voltage till the initiation of the sparking on the surface, (c) the insulator surface after the sparking experiment and the maximum working voltage.

#### 4. CONCLUSIONS

Due to the importance of electricity in all areas of daily life and various industries, a short-term power outage can cause significant damage. To solve this problem, this study, for the first time, examines a practical solution to increase the efficiency of the operating insulators on power lines. This study aims to create a hydrophobic surface on insulators, which causes the insulator to be self-clean, and increases its lifetime and also its efficiency. The coating studied in this research is stabilized and used at ambient temperature without using heat treatments. This can prevent power outages by repairing the insulators. Silica, the main material used to create this hydrophobic coating, is a low-cost and available material in the industry and it has increased the breakdown voltage of the insulator used from 62 kV to 72 kV. The contact angle between the water and the coated surface with the synthesized hydrophobic nano-silica was measured at 149 degrees. This indicates the acceptable hydrophobicity of this coating in environmental conditions. Also, the lifetime of the created coating is 9 months in harsh environmental conditions and intense UV radiation of sunlight.

#### REFERENCES

- [1] Yao, T., "Preparation of super hydrophobic coating for insulator against icing flashover." in 2017 2nd International Conference on Materials Science, Machinery and Energy Engineering (MSMEE 2017). 2017. Atlantis Press.
- [2] Vallabhuneni, S., Movafaghi, S., Wang, W. and Kota, A.K., "Superhydrophobic Coatings for Improved Performance of Electrical Insulators." *J. Macromolecular Materials and Engineering.*, 2018, 303(9), 1800313.
- [3] Peng, W., Gou X., Qin, H., Zhao, M., Zhao, X. and Guo, Zh., "Creation of a multifunctional superhydrophobic coating for composite insulators." *J. Chemical Engineering.*, 2018, 352, 774-781.
- [4] Li, J., Zhao, Y., Hu, Jianlin., Shu, L. and Shi, X., "Anti-icing performance of a superhydrophobic PDMS/modified nano-silica hybrid coating for insulators." *J. Adhesion Science and Technology*, 2012, 26(4-5), 665-679.
- [5] Gençoğlu, M.T., "The comparison of ceramic and non-ceramic insulators." *J. Engineering Sciences*, 2007, 2(4), 274-294.
- [6] Darmanin, Th. and Guittard, F., "Superhydrophobic and superoleophobic properties in nature". *J. Materials today*, 2015, 18(5), 273-285.
- [7] Solga, A., Cerman, Z., Striffler, B.F., Spaeth, M. and Barthlott, W., "The dream of staying clean: Lotus and biomimetic surfaces." *J. Bioinspiration & biomimetics*, 2007, 2(4), S126.
- [8] Berrada, N., Hamze, S., Desforges, A., Ghanbaja, J., Gleize, J., Maré, Th., Vigolo, B. and Estellé, P., "Surface tension of functionalized MWCNT-based nanofluids in water and commercial propylene-glycol mixture." *J. Molecular Liquids*, 2019, 293, 111473.
- [9] Jang, G.M. and Il Kim, N., "Surface tension, light absorbance, and effective viscosity of single droplets of water-emulsified n-decane, n-dodecane, and n-hexadecane." *J. Fuel*, 2019, 240, 1-9.
- [10] Ganesh, V.A., Raut, H.K., Sreekumar Nair, A., and Ramakrishna S., "A review on self-cleaning coatings." *J. Materials Chemistry*, 2011, 21(41), 16304-16322.
- [11] Blossey, R., "Self-cleaning surfaces—virtual realities." *J. Nature materials*, 2003, 2(5), 301.
- [12] Nakamura, I., Negishi, N., Kutsuna, Sh., Ihara, T., Sugihara, Sh. and Koji Takeuchi, "Role of oxygen vacancy in the plasma-treated TiO<sub>2</sub> photocatalyst with visible light activity for NO removal." *J. Molecular Catalysis A: Chemical*, 2000, 161(1-2), 205-212.
- [13] Li, Y. and Somorjai, G.A., "Nanoscale advances in catalysis and energy applications." *J. Nano letters*, 2010, 10(7), 2289-2295.
- [14] Notsu, H., Kubo, W., Shitanda, Isao. and Tatsuma, T., "Super-hydrophobic/superhydrophilic patterning of gold surfaces by photocatalytic lithography." *J. Materials Chemistry*, 2005, 15(15), 1523-1527.
- [15] Aytug, T., Lupini, A.R., Jellison, G.E., Joshi, P.C., Ivanov, I.H., Liu, T., Wang, P., Menon, R., Trejo, R.M., Lara-Curzio E., Hunter S.R., Simpson, J.T., Paranthaman,

- M.P and Christena DKK, "Monolithic graded-refractive-index glass-based antireflective coatings: broadband/omnidirectional light harvesting and self-cleaning characteristics." *J. Materials Chemistry C*, 2015, 3(21), 5440-5449.
- [16] Chen, L., Sun, X., Hang, J., Jin, L., Shang, D., and Shi, L., "Large- Scale Fabrication of Robust Superhydrophobic Coatings with High Rigidity and Good Flexibility." *J. Advanced Materials Interfaces*, 2016, 3(6), 1500718.
- [17] Baghshahi, S., Mohammadi, M., Payrazm, S. and Aliabadizadeh, A., "Hydrophobic nanocrystalline glazes based on cassiterite for self-cleaning outdoor power grid insulators." *J. European Ceramic Society*, 2021, 41, 5750-5754.